



Published in final edited form as:

*Congenit Anom (Kyoto)*. 2019 May ; 59(3): 93–98. doi:10.1111/cga.12303.

## Identification and association of recurrent *ALOXE3* mutation with non-bullous congenital ichthyosiform erythroderma in two ethnically distinct Pakistani families

Simeen Ber Rahman<sup>1</sup>, Asif Mir<sup>2</sup>, Nafees Ahmad<sup>3</sup>, Syed Husnain Haider<sup>3</sup>, Salman Akbar Malik<sup>4</sup>, and Muhammad Nasir<sup>3</sup>

<sup>1</sup>Dr. Simeen's Aesthetic Skin & Laser Clinic, Rawalpindi, Pakistan

<sup>2</sup>Department of Biotechnology, International Islamic university, Islamabad, Pakistan

<sup>3</sup>Institute of Biomedical and Genetic Engineering, 24-Mauve area, G-9/1 Islamabad 44000, Pakistan

<sup>4</sup>Department of Biochemistry, Quaid-i-Azam University, Islamabad 44000, Pakistan

### Abstract

Non-bullous congenital ichthyosiform erythroderma (NCIE) is characterized by skin scaling with erythema. In this study, two Pakistani families with NCIE are genetically characterized through Whole Exome and Sanger sequencing to identify molecular basis of the disease. We identified a nonsense homozygous c.2026C>T mutation of *ALOXE3*, causing premature termination of the eLOX3 protein (p.Q676X). *In silico* studies predicted impaired enzymatic activity of the premature truncated eLOX3, leading to abnormal synthesis of specific hepxilin derivatives, essential for epidermal barrier formation. It is the first ever study reporting homozygotes of p.Q676X mutation in ethnically distinct two Pakistani families; otherwise, heterozygotes of the said mutation have been reported in South Asian population only. Hence, mutation seems to be region-specific and may be useful for molecular diagnosis of NCIE. Moreover, our findings should help in genetic counseling and career screening.

### Keywords

Autosomal recessive congenital ichthyosis; non-bullous congenital ichthyosiform erythroderma; eLOX3; impaired epidermal formation

### Introduction

Autosomal recessive congenital ichthyoses (ARCI) is a rare heterogeneous group of keratinization disorders (Richard & Bale, 1993). Recently, three major subtypes of ARCI has been described; spectrum of lamellar ichthyoses (LI), congenital ichthyosiform

**Correspondence:** Dr. Muhammad Nasir, Ph D. Institute of Biomedical and Genetic Engineering, 24-Mauve area, G-9/1, Islamabad, Pakistan, Ph: +92-51-9106281, Fax: +92-51-9106283, nasirmalik\_soonvalley@yahoo.com.

**Conflict of interest:** None

erythroderma (CIE)/non-bullous congenital ichthyosiform erythroderma (NCIE) and the highly lethal congenital harlequin ichthyosis (HI) (Louhichi et al., 2013). Among subtypes, NCIE is specific type of ARCI with ~ 90% of the infants are born encased in a collodion membrane, a tight shiny membrane that resembles plastic wrap (Fischer et al., 2000). Clinically, patients with NCIE exhibit fine white scales in addition to variable generalized erythroderma. Some patients may have ectropion, eclabium, scalp alopecia, nail dystrophy and decreased sweating with heat intolerance (Choudhary & Satish, 2015).

To date, at least twelve different genes; *ABCA12*, *ALOX12B*, *ALOXE3*, *CASP14*, *CERS3*, *CYP4F22*, *LIPN*, *NIPAL4*, *PNPLA1*, *SDR9C7*, *SLC27A4* and *TGM1* are described to be associated with ARCI. Of which, *ALOXE3* and *ALOX12B* are typically implicated in NCIE pathogenesis (Richard & Bale, 1993). Interestingly, the cases of ARCI/NCIE involving *ALOXE3* are very rare, with less than 30 families have been reported in the literature so far (Sugiura & Akiyama, 2015). *ALOXE3* and *ALOX12B* encode epidermis-type lipoxygenase 3 (eLOX3) and arachidonate 12-lipoxygenase, 12R type (2R-LOX) respectively. Both proteins are functionally allied, constitute LOX pathway (12R-LOX–eLOX3 pathway) that regulates terminal differentiation of keratinocytes and formation of the epidermal lipid barrier (Eckl et al., 2005). The 12R-LOX catalyzes arachidonic acid conversion into 12R-hydroxyeicosatetraenoic acid (12R-HETE) to generate fatty acid hydroperoxide. Whereas, eLOX3 functions as a hydroperoxide isomerase and oxidizes these intermediate products into specific epoxy alcohol, 8R-hydroxy-11R, 12R-epoxyeicosa-5Z,9E,14Z-trienoic acid, essential for lipid barrier formation (Yu et al., 2007).

## Materials and Methods

The Ethical Committee of Institute of Biomedical and Genetic Engineering (IBGE), Islamabad, Pakistan reviewed and approved the study protocols (Ref. No. IBGE/IEC/18/01/16). The study was conducted in accordance with the principles of declaration of Helsinki.

### Sample collection and processing

Ethnically different two Pakistani families with ARCI, labeled as Family A and Family B have participated in the study. Participants, including affected and unaffected individuals in families as well as 100 ethnically-matched unrelated normal individuals, were consented to the study and blood samples were collected. Genomic DNA was extracted by standard phenol–chloroform extraction method (Sambrook et al., 1989).

### Whole Exome and Sanger Sequencing

Whole exome sequencing of index cases was performed on Illumina HiSeq2000. Sequence was aligned to the human genome reference (UCSC Genome Browser, hg19) with the Burrows-Wheeler Aligner (BWA-MEM). Processing of aligned reads was performed in accordance to GATK best practices. Variants were annotated by employing AnnoVar.

Sanger sequencing was used to confirm identified SNVs as described previously (Nasir et al., 2011).

## Bioinformatics Analysis

Prediction of secondary structure features was done using Psipred (<http://bioinf.cs.ucl.ac.uk/psipred/>) and for tertiary structure, modeling I-Tasser (<https://zhanglab.ccmb.med.umich.edu/I-TASSER/>) was used. RAMPAGE server confirmed the accuracy of models (<http://mordred.bioc.cam.ac.uk/~rapper/rampage.php>). Pockets on 3D structures of proteins were identified using CASTp server (<http://sts.bioe.uic.edu/castp/view/viewer2.php>). STITCH4 database (<http://stitch.embl.de/>) was used for prediction of functional interactive partners of protein. Docking was done using PatchDock server (<https://bioinfo3d.cs.tau.ac.il/PatchDock/>). Protein-ligand interaction complexes were analyzed and represented through LIGPLOT (<https://www.ebi.ac.uk/thornton-srv/software/LIGPLOT/>).

## Results

### Clinical Findings

Six affected individuals (age's ranges from 4-35 years) from both families displayed typical signs and symptoms of ichthyosis that started appearing during their infancy. However, there was remarkable clinical heterogeneity was observed, not only between the families but also within a family. Family A reported collodion babies while Family B did not report presence of collodion membrane in affected infants. Skin scaling on erythematic background was a common finding but severity of erythema and pattern of scaling was quite different within and between families. Facial fine, whitish superficial scales on profound erythema were observed in Family A (Fig. 1a,e) as compare to mild erythema in affected individuals of Family B (Fig. 1i).

Within Family A, overall intensity of erythema and hyperkeratosis was higher in individual V:2 (Fig. 1e,f,g) than individual V:1 (Fig. 1a,b,c). Likewise, Individual V:2 was presented with larger brown adherent scales (Fig. 1h) as compare to smaller light brown adherent scales noted in individual V:1 (Fig. 1d). Affected individuals from Family B were presented with fine, whitish superficial scales on face without prominent erythema. Generalized semi adherent coarse brown scaling was present on whole body. Hyperkeratosis on different body parts including armpit, elbow, feet etc was also noted (Fig. 1j-l). No ectropion or eclabium, scalp alopecia and nail dystrophy were noted. Height to weight ratio were in normal range according to appropriate age group.

Based on medical history, presence of significant erythema and scaling, a preliminary diagnosis of non-bullous congenital ichthyosis erythroderma was made.

### Genetic Screening

Pedigree analysis of was strongly suggestive of autosomal recessive mode of inheritance in both families (Fig. 2a). Exome sequencing of index cases revealed a homozygous nonsense mutation c.2026C>T in exon 13 of the *ALOXE3* gene, causing substitution of serine with a stop codon (TAG).

Sanger sequencing revealed heterozygous carrier status of parents from both families (Fig. 2b) while affected subjects were found with homozygous status for c.2026C>T variation

(Fig. 2c). The identified genetic variation was not found in 100 ethnically matched unrelated healthy control samples.

### ALOXE3 Sequence Analysis and Structure Prediction

Secondary structure features of normal ALOXE3 protein include 23 helices, 15 strands, and 38 coils (Fig. 3a) while mutant (p.Q676X) predicted 16 helices, 16 strands and 33 coils (Fig. 3b). Chemical ligand baicalein with maximum interaction score (0.869) for ALOXE3 was predicted and selected as an interactive partner for molecular docking analysis. 3D visualization of docking complex between baicalein and wild-type/mutant (p.Q676X) ALOXE3 has been shown in Figure 3c.

Hydrophobic and hydrogen bonding interactions of docked molecules were compared using LigPlot program. Ligplot output for the interactions is shown in Figure 4a and 4b for normal and mutant dockings, respectively. In normal protein, there were total 142 interaction sites and residues involved in docking interaction lies in pocket number 139, while 82 pockets were predicted in mutant protein and interacting residues belong to pocket number 81. Hence, mutation resulted in change of total number of pockets and specific active sites involved in normal protein docking (Table 1).

### Discussion

A central aspect of epidermal barrier formation is the fusion of lipid-enriched lamellar bodies with terminally differentiating keratinocyte plasma membrane and extrusion of lipid contents in the upper keratinocyte layers (Hanel et al., 2013). These lipid precursors are processed through 12R-LOX–eLOX3 pathway to produce specific hepxilin derivatives (fatty acid epoxy alcohols). Such intermediate products trigger physiological responses by binding and activating peroxisome proliferator-activated receptors (PPARs) which regulates expression of target genes, hence stimulate keratinocytes proliferation/differentiation and skin development (Michalik & Wahli, 2008, Yu et al., 2003). Since lipoxygenase genes, *ALOX12B* and *ALOXE3* closely regulate 12R-LOX–eLOX3 pathway; therefore, pathogenic variations in either of the gene may interrupt normal pathway, leading to abnormal skin development (Eckl, Krieg, Kuster, Traupe, Andre, Wittstruck, Furstenberger & Hennies, 2005).

Despite diverse clinical presentation, in the present study, patients from both families revealed a homozygous nonsense c.2026C>T mutation in exon 13 of the *ALOXE3* which led to the conversion of serine amino acid into a stop codon at position 676 (p.Q676X). The identified mutation has been described in South Asian population only with an allele count 6 and population frequency as 0.0003635 (<http://exac.broadinstitute.org/variant/17-8011840-G-A>); however, no homozygote for this mutation is reported so far. This is the first ever family-based study describing the homozygous status of this nonsense mutation in two ethnically distinct Pakistani families and explains its association with NCIE. Before this, 5 recurrent mutations including p.Arg119GlyfsX12 in exon 3, p.Arg234X and p.Lys240ArgfsX40 in exon 6, p.Gln344\_Ala347delinsPro in exon 8, p.Pro630Leu in exon 14 of *ALOXE3* has been described (Eckl et al., 2009). However, the identified recurrent mutation p.Q676X belongs to exon 13 of the *ALOXE3* gene.

The identified p.Q676X mutation was tested against different bioinformatics tools to assess its impact on protein structure, function as well as protein interaction kinetics. It was predicted that nonsense mutation significantly affected the number of secondary structure features of the protein including helices, strands, coils etc and changed the protein interaction kinetics. Considerable difference in number and position of residues and atoms involved in interaction during docking process (Table 1) of normal and mutant types suggest that identified nonsense p.Q676X mutation have significantly affected protein structure as well as its conformation and interaction characteristics. Hence, defective eLOX3 might have led to reduced or impaired isomerase activity to generate 12R-HETE-derived epoxy alcohol metabolites essential for normal skin barrier function. Moreover, there may be a complete loss of eLOX3 protein expression through nonsense-mediated mRNA decay (NMD) or transcription initiation failures (Peccarelli & Kebaara, 2014), leading to defective skin formation with NCIE.

In summary, the present study not only expands the spectrum of families involving NCIE pathogenesis but also the body of evidences supporting the role of eLOX3 in normal skin barrier formation. Identification of recurrent mutation in two Pakistani families may possibly be a founder effect; however, its occurrence, though in heterozygous status, in some other random individuals from South Asian populations suggests the mutation possibly region-specific and that the site is relatively mutable. The identified recurrent mutation is an addition to the spectrum of previously reported five recurrent mutations of ALOXE3. In future, it may be helpful for molecular diagnosis of NCIE and screening of ALOXE3 in additional samples will be supportive in this regard. At present, our findings may be supportive for prenatal genetic screening and early diagnosis of NCIE/ARCI.

## Acknowledgments

We would like to thank the patients and their family members who contributed in this study. The work was supported in part by IBGE, Islamabad, Pakistan, HEC, Pakistan (IRSIP 25 BMS 10), NIH, USA (R01AR068392 to Keith Adam Choate, Departments of Dermatology, Yale University, New Haven, CT 06519 USA, and Yale Centre for Mendelian Genomics U54 HG006504). All these sources provided support for the conduct of research only.

## References

- Choudhary R, Satish V. 2015; Dental Treatment of a Child Suffering from Non-bullous Congenital Ichthyosiform Erythroderma under General Anesthesia. *Int J Clin Pediatr Dent.* 8:157–62. [PubMed: 26379388]
- Eckl KM, de Juanes S, Kurtenbach J, et al. 2009; Molecular analysis of 250 patients with autosomal recessive congenital ichthyosis: evidence for mutation hotspots in ALOXE3 and allelic heterogeneity in ALOX12B. *The Journal of investigative dermatology.* 129:1421–8. [PubMed: 19131948]
- Eckl KM, Krieg P, Kuster W, et al. 2005; Mutation spectrum and functional analysis of epidermis-type lipoxygenases in patients with autosomal recessive congenital ichthyosis. *Human mutation.* 26:351–61. [PubMed: 16116617]
- Fischer J, Faure A, Bouadjar B, et al. 2000; Two new loci for autosomal recessive ichthyosis on chromosomes 3p21 and 19p12-q12 and evidence for further genetic heterogeneity. *American journal of human genetics.* 66:904–13. [PubMed: 10712205]
- Hanel KH, Cornelissen C, Luscher B, Baron JM. 2013; Cytokines and the skin barrier. *International journal of molecular sciences.* 14:6720–45. [PubMed: 23531535]

- Louhichi N, Hadjsalem I, Marrakchi S, et al. 2013; Congenital lamellar ichthyosis in Tunisia is caused by a founder nonsense mutation in the TGM1 gene. *Molecular biology reports*. 40:2527–32. [PubMed: 23192619]
- Michalik L, Wahli W. 2008; PPARs Mediate Lipid Signaling in Inflammation and Cancer. *PPAR Res*. 2008:134059. [PubMed: 19125181]
- Nasir M, Latif A, Ajmal M, et al. 2011; Molecular analysis of lipoid proteinosis: identification of a novel nonsense mutation in the ECM1 gene in a Pakistani family. *Diagn Pathol*. 6:69. [PubMed: 21791056]
- Peccarelli M, Kebaara BW. 2014; Regulation of natural mRNAs by the nonsense-mediated mRNA decay pathway. *Eukaryot Cell*. 13:1126–35. [PubMed: 25038084]
- Richard, G, Bale, SJ. Autosomal Recessive Congenital Ichthyosis. In: Pagon, RA, Adam, MP, Ardinger, HH. , et al., editors. *GeneReviews(R)*. Seattle (WA): 1993.
- Sambrook, J, Fritsch, EF, Maniatis, T. *Molecular cloning: a laboratory manual*. Cold spring harbor laboratory press; 1989.
- Sugiura K, Akiyama M. 2015; Lamellar ichthyosis caused by a previously unreported homozygous ALOXE3 mutation in East Asia. *Acta Derm Venereol*. 95:858–9. [PubMed: 25423909]
- Yu Z, Schneider C, Boeglin WE, Brash AR. 2007; Epidermal lipoxygenase products of the hepoxilin pathway selectively activate the nuclear receptor PPARalpha. *Lipids*. 42:491–7. [PubMed: 17436029]
- Yu Z, Schneider C, Boeglin WE, Marnett LJ, Brash AR. 2003; The lipoxygenase gene ALOXE3 implicated in skin differentiation encodes a hydroperoxide isomerase. *Proceedings of the National Academy of Sciences of the United States of America*. 100:9162–7. [PubMed: 12881489]



**Figure 1. Clinical presentation of affected individuals with NCIE**

(a) Subject V: 1, Family A; 7-years old female displays fine white, superficial scales with prominent erythema (b,c) Hyperkeratosis on dorsum of the neck and hand respectively (d) Small light brown, less adherent scales around trunk. (e) Subject V: 2, Family A; a 1-year old female presents fine white, superficial, scales with profound erythema on face. (f,g) Hyperkeratosis on neck and hand respectively (h) Large, brown adherent scales around trunk. (i) Subject IV: 2, Family B; a 35-years old male shows fine white, superficial scales on face with mild erythema (j) whitish to brown, coarse adherent scales on trunk and (k,l) marked hyperkeratosis on different body parts; around armpit, elbow, feet etc. Permission has been obtained from patients and their family for presentation.

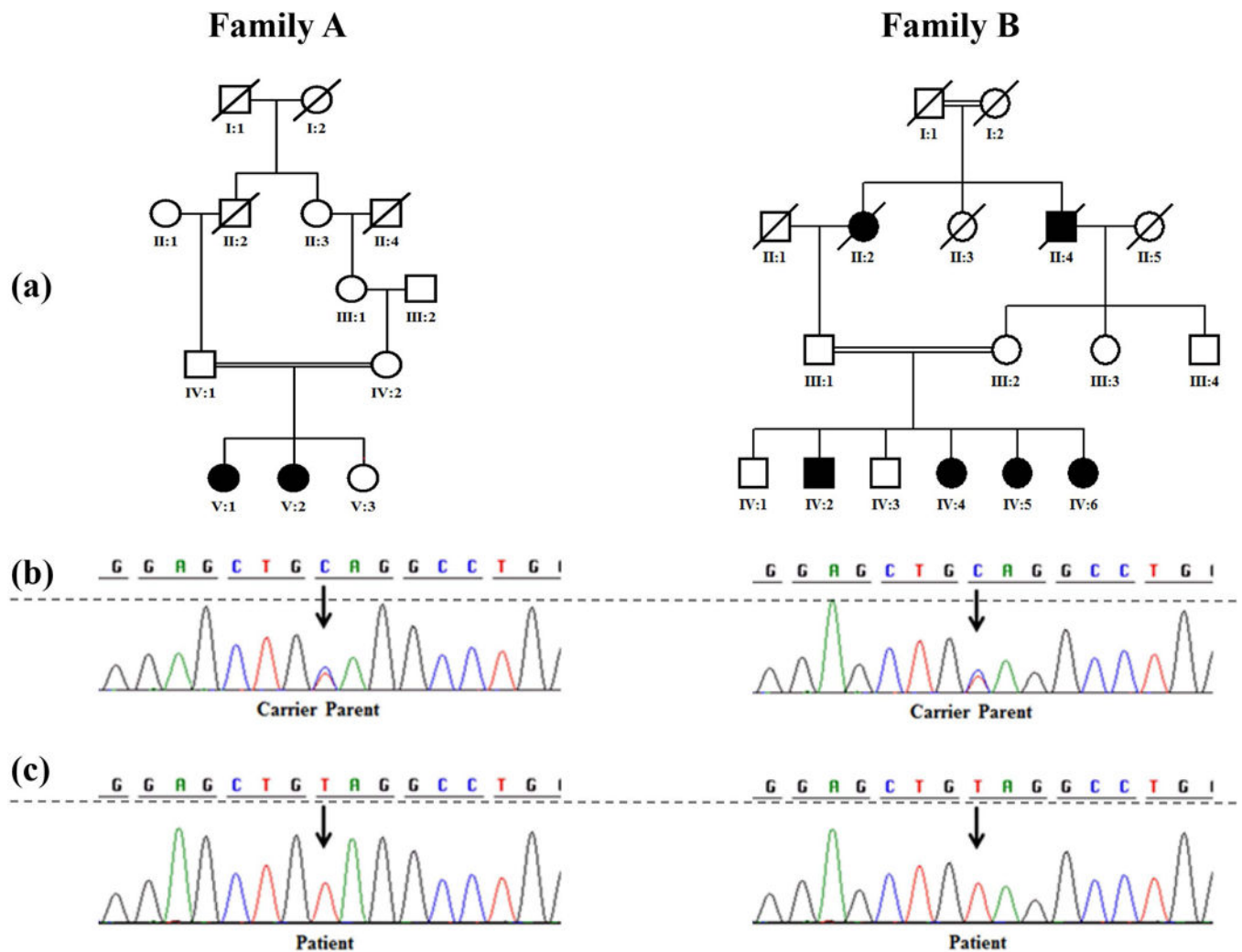


**Figure 2. Pedigrees of ARCI families and Sanger Sequencing of *ALOXE3* gene**  
 Panel (a) shows pedigrees of two consanguineous multigenerational Pakistani families with ARCI. Panel (b and C) illustrates Sanger sequencing of carrier parents and affected subjects respectively, from both ARCI families. Arrow identifies the site of mutation with heterozygous condition (C/T) in carrier parents while homozygous status (T/T) in patients for the mutant allele.

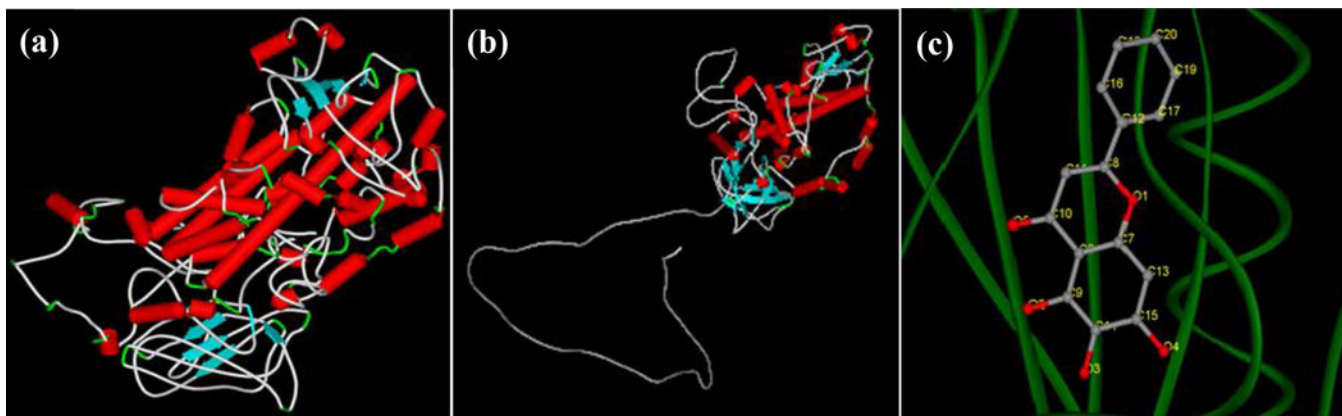


**Figure 3. 3D Predicted Models**

a) Normal ALOXE3 showing structure features b) Mutant ALOXE3 (p.Q676X). In Part A and B, Red cylinders shows  $\alpha$ -helix, Flattened cyan arrows represents  $\beta$ -Sheets and wire like structure is representing Loops. c) Visualization of docking complex (ALOXE3 Vs Baicalein); Receptor: Green Color & Solid Ribbon Display Style, Ligand: Ball & Stick Display Style with Atoms labeled in yellow.

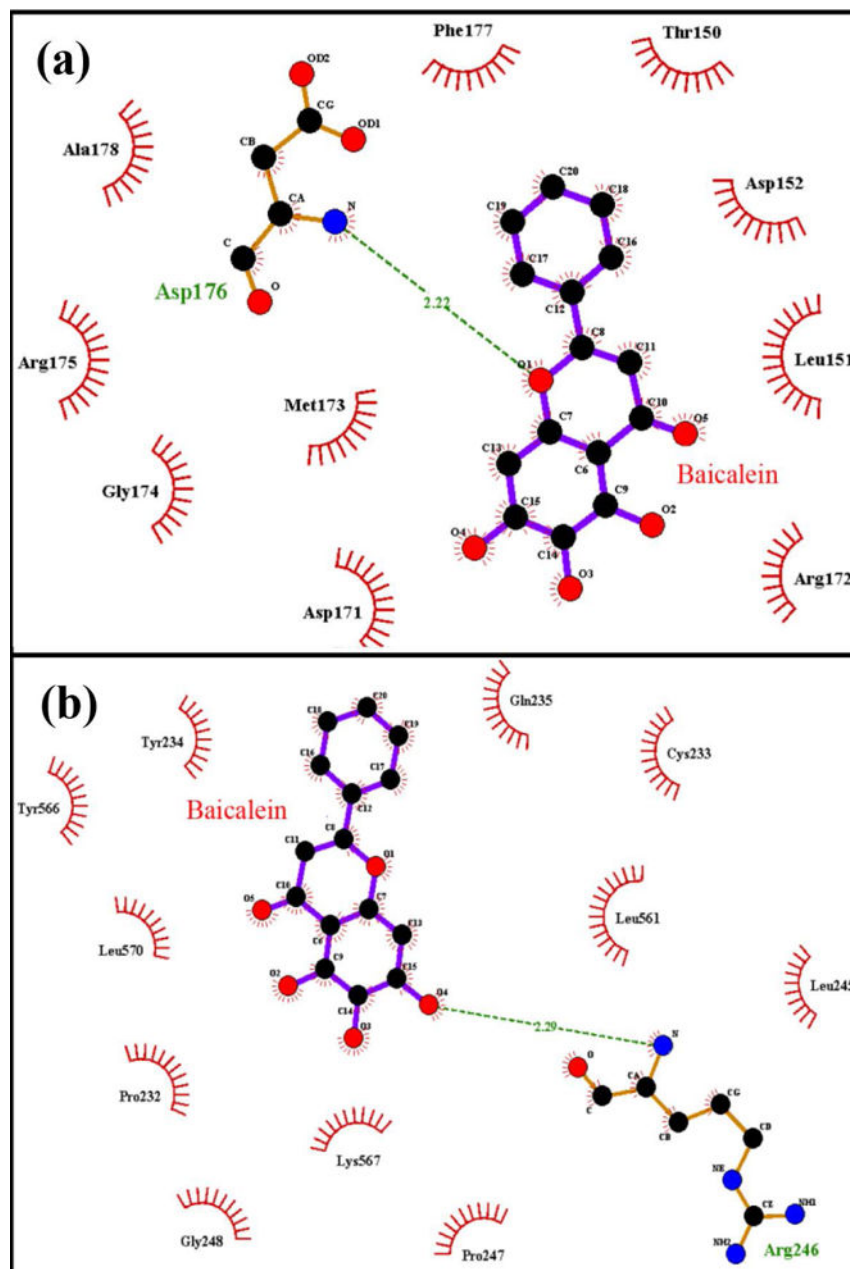


**Figure 4. 2D Ligplot representation of Docking Interactions**

a) Normal ALOXE3 with Baicalein. b) Mutant ALOXE3 (p.Q676X) vs Baicalein. Receptor Residues Involved in Hydrophobic Interactions are represented by brick red spoked arcs (  ), Hydrogen Bonding shown by Green dotted lines ( ..... ). Receptor residues involved in H-Bonding written in Olive Green Color.

Table 1

Docking Interactions: residues and atoms involved are summarized.

| Receptor-Ligand                    | Hydrogen Bond Interactions |                   | Hydrophobic Interactions   |   | Figure |
|------------------------------------|----------------------------|-------------------|--|---|--------|
|                                    | Ligand Atoms               | Receptor Residues | Ligand Atoms   | Receptor Residues   |        |
| <b>Wild-type ALOXE3- Baicalein</b> | O <sub>1</sub>             | Asp176            | O <sub>1</sub> , O <sub>3</sub> , O <sub>4</sub> , O <sub>5</sub> , C <sub>6</sub> ,<br>C <sub>7</sub> , C <sub>8</sub> , C <sub>10</sub> , C <sub>11</sub> ,<br>C <sub>12</sub> , C <sub>13</sub> , C <sub>14</sub> , C <sub>15</sub> ,<br>C <sub>16</sub> , C <sub>17</sub> , C <sub>18</sub> , C <sub>19</sub> ,<br>C <sub>20</sub>                 | Thr150, Leu151,<br>Asp152, Asp171,<br>Arg172, Met173,<br>Gly174, Arg175,<br>Phe177, Ala178            | 4A     |
| <b>Mutant ALOXE3-Baicalein</b>     | O <sub>4</sub>             | Arg246            | O <sub>1</sub> , O <sub>2</sub> , O <sub>3</sub> , O <sub>4</sub> , O <sub>5</sub> ,<br>C <sub>6</sub> , C <sub>7</sub> , C <sub>8</sub> , C <sub>9</sub> , C <sub>10</sub> ,<br>C <sub>12</sub> , C <sub>13</sub> , C <sub>14</sub> , C <sub>15</sub> ,<br>C <sub>16</sub> , C <sub>17</sub> , C <sub>18</sub> , C <sub>19</sub> ,<br>C <sub>20</sub> | Pro232, Cys233,<br>Tyr234, Gln235,<br>Leu245, Pro247,<br>Gly248, Leu561,<br>Tyr566, Lys567,<br>Leu570 | 4B     |